Spatial Instability of the Barotropic Jet with Slow Streamwise Variation

MELINDA S. PENG AND R. T. WILLIAMS

Department of Meteorology, Naval Postgraduate School, Monterey, CA 93943

(Manuscript received 23 October 1985, in final form 8 May 1986)

ABSTRACT

A two-scale expansion technique is used to study the barotropic instability of basic flows with slow streamwise variation. Disturbances in nonparallel flow possess properties that differ from those calculated from parallel flow theory. The difference, which is obtained at higher order in the parameter that measures the nonparallelism, depends on the first derivative of the parallel flow properties with respect to the streamwise direction. This higher order correction shifts the spatial growth rate profile for the nonparallel flow downstream relative to the spatial growth rate profile for parallel flow. These results are compared with a previous numerical study by Tupaz, Williams and Chang, and some of their conclusions are modified.

Physically, the difference in the spatial instability for parallel and nonparallel flow is subject to two combined effects. The first is the lag effect discussed by Tupaz et al., which causes the disturbance structure to lag the parallel-flow solution structure in regions where the mean flow changes rapidly downstream. This causes the downstream shifting of the nonparallel growth rate profile. The second is related to the phase speed difference between the parallel and nonparallel flows. If the disturbance propagates faster than predicted by the parallel flow theory, the local spatial growth rate will be smaller than that calculated by the parallel flow and vice versa.

1. Introduction

Barotropic and baroclinic instabilities that are characterized by horizontal shear and vertical shear, respectively, are the principal instabilities of large-scale atmospheric flows. Conventionally, the instability of a sheared flow is studied by assuming that the mean flow is uniform (parallel) in the streamwise direction. Yet, in reality the mean flows are frequently nonparallel. An example is the subtropical jet stream, which has much stronger baroclinic shear near Japan and much weaker shear to the west and east (Krishnamurti, 1961). It is common to predict the linear growth rate of the synoptic scale waves based on the temporal instability of the parallel flow without considering the influence of the streamwise variation. Therefore, the regions with strongest shear are expected to be the most unstable and to be the most favorable places for the disturbances to grow. However, if the disturbances propagate with a relatively fast speed, the local instability may not be achieved as the disturbances propagate through a spatially varying mean flow. Tupaz et al. (1978; hereafter referred to as TWC) and Williams et al. (1984) found the spatial-growth approach to be very attractive for the study of barotropic jets with streamwise variation. With this approach it is assumed that a train of waves of constant amplitude move into the region of interest from the upstream side. This is equivalent to having a periodic forcing on the upwind boundary as was employed by TWC. As the waves move into the region of interest they grow spatially in response to the streamwise changes in the mean flow. (Their time variation is periodic.) If the temporal instability approach is used, cyclic boundary conditions are required and a single temporal growth rate is obtained. In order to get the effects of streamwise mean flow variations, the streamwise variations in the eigensolution must be analyzed. With the spatial growth approach, variations in spatial growth rate can be directly related to variations in the mean flow. The amplifying modes have been regarded since the early 1960s as physically superior to unstable modes in describing the shear instabilities. For example, the eigenvalue problem solved for amplifying waves in a shear flow by Michalke (1965) gave better agreement with experimental observations. Later, this approach was successfully extended to strong nonlinear developments. A discussion of relevant literature can be found in Merkine (1977).

TWC used a numerical model to study the nonparallel linear barotropic instability. The basic flow was a Bickley jet that roughly simulates the easterly jet observed south of the Tibetan high near 200 mb during Northern Hemispheric summer. Two major results were obtained by them. First, it was found that the maximum spatial growth rate for nonparallel flow was about 25% larger than that calculated from the parallel flow theory. Second, the location of the maximum growth rate region was shifted downstream from where the parallel flow predicted the local maximum. This downstream shifting corresponds to the lag of the spatial structure of the disturbance in nonparallel flow that was discussed by TWC. The maximum of the wave-

packet is further shifted downstream of the maximum shear region where the spatial growth rate vanishes. In a similar numerical study for weakly nonparallel barotropic flow with a localized potential vorticity source, Merkine and Balgovind (1983) also observed the downstream shifting of the maximum wavepacket.

From observations, the variation of the basic flow in the streamwise direction is usually much slower than the variation in the cross current direction. This suggests that the variation of the basic flow can be separated into different scales in space so that an analytical formulation will be tractable. The purpose of the present study is to examine the effect of the downstream variation of a jet on its stability properties using a multiple-scale expansion technique. Benney and Rosenblat (1964) developed the procedure for the analytical formulation for the stability of spatially varying and time-dependent flows, and a similar approach was used by Drazin (1974) for several model studies. Their ideas and those of Nayfeh et al. (1974) and Saric and Nayfeh (1975) will be used in the present study.

The basic model is described in section 2, and the mathematical formulations for the multiple-scale expansion are developed in section 3. In section 4, the relationship between temporal and spatial growth rate is discussed and some of the conclusions from TWC are modified. The results are presented in section 5. Section 6 contains the concluding remarks.

2. The model

The model treats the barotropic instability of a zonal jet confined within a channel in the east–west direction. As in TWC, the nondivergent barotropic vorticity equation is used. In a linearized nondimensional form, this equation can be written as

$$\frac{\partial}{\partial t}\nabla^2\psi' - \frac{\partial\bar{\psi}}{\partial y}\frac{\partial}{\partial x}\nabla^2\psi' + \frac{\partial\bar{\psi}}{\partial x}\frac{\partial}{\partial y}\nabla^2\psi' - \frac{\partial\psi'}{\partial y}\frac{\partial}{\partial x}\nabla^2\bar{\psi} + \frac{\partial\psi'}{\partial x}\frac{\partial}{\partial y}\nabla^2\bar{\psi} + \beta\frac{\partial\psi'}{\partial x} = -\lambda\nabla^2\psi' \quad (2.1)$$

where ψ' and $\bar{\psi}$ are the disturbance and basic state streamfunctions, respectively, and the nondivergent velocity components are

$$\left.\begin{aligned} u &= -\frac{\partial\psi'}{\partial y}, \quad v = \frac{\partial\psi'}{\partial x} \\ \bar{U} &= -\frac{\partial\bar{\psi}}{\partial y}, \quad \bar{V} = \frac{\partial\bar{\psi}}{\partial x} \end{aligned}\right\}. \quad (2.2)$$

The north and south boundaries are placed at $y = \pm Y$, where the disturbance streamfunction ψ' vanishes, i.e.,

$$\psi' = 0, \quad y = \pm Y. \quad (2.3)$$

The following relate the nondimensional and dimensional (denoted by an asterisk) forms of the variables:

$$\left.\begin{aligned} x^* &= Dx \\ y^* &= Dy \\ U^* &= U_{\max}U \\ T^* &= \frac{D}{U_{\max}}t \\ \beta^* &= \frac{U_{\max}}{D^2}\beta \\ \lambda^* &= \frac{U_{\max}}{D}\lambda \\ \psi^* &= DU_{\max}\psi \end{aligned}\right\} \quad (2.4)$$

Since we are considering basic flow whose streamwise variation is slow compared to its variation in the cross-stream direction, a small parameter ϵ is defined as the ratio between the characteristic length scale of the basic flow in the cross-stream (y) direction, D, and the characteristic length scale in the streamwise (x) direction, L:

$$\epsilon = \frac{D}{L} \ll 1. \quad (2.5)$$

This allows us to introduce a slow scale in the x-direction

$$x_1 = \epsilon x. \quad (2.6)$$

For a truly parallel flow, $L \to \infty$ and $\epsilon = 0$. For the nonparallel flow, the basic flow is a function of x_1 and y. The flow profile has the form of a Bickley jet, with $\bar{U}$ and $\bar{V}$ fields prescribed as

$$\bar{U}(x_1, y) = -\frac{\partial\bar{\psi}}{\partial y} = U(x_1)\,\mathrm{sech}^2\left(\frac{y}{d(x_1)}\right) + u_0, \quad (2.7)$$

$$\bar{V}(x_1, y) = \frac{\partial\bar{\psi}}{\partial x} = \epsilon\frac{\partial\bar{\psi}}{\partial x_1} \quad (2.8)$$

where $d(x_1)$ is the half-width of the jet and $U(x_1)$ is the maximum wind speed across the jet at a particular x_1. The basic flow has the same profile as in TWC, so the results can be compared. The streamwise variation of the basic flow arises from the following variations in $U(x_1)$ and $d(x_1)$:

$$d(x_1) = 0.85 + 0.35\cos(x_1 + \pi), \quad (2.9)$$

$$U(x_1) = \frac{0.5}{d(x_1)}\coth\left(\frac{2}{d(x_1)}\right). \quad (2.10)$$

The characteristic values chosen for $U_{\max}$, D, L, β and λ are

$$\left.\begin{aligned} U_{\max} &= -30\ \mathrm{m\ s^{-1}} \\ D &= 1000\ \mathrm{km} \\ L &= 10\,000\ \mathrm{km} \\ \epsilon &= 0.1 \\ \beta &= 2\Omega(\cos 10°)/a \\ \lambda &= 0.15 \times 10^{-5}\ \mathrm{s^{-1}} \end{aligned}\right\} \quad (2.11)$$

where a is the radius of the earth and Ω is the angular velocity of the earth's rotation. The nondimensional width of the channel is equal to $2Y = 4$, and the streamwise variation is considered within $-2.0 \leqslant x_1 \leqslant 2.0$. Equations (2.9) and (2.10) show that the variation of the basic flow is symmetric with respect to $x_1 = 0$. The north–south profiles of $\bar{U}$ at several streamwise locations are given in Fig. 1.

3. Solution procedure

With the introduction of (2.5)–(2.8), the coefficients in (2.1) are independent of x and t; the normal-mode solution, which has a significant growth rate, is of the form

$$\psi' = \phi(x_1, y)e^{i\theta} \tag{3.1}$$

where θ is the phase of the normal mode. The phase is related to the wavenumber k and frequency ω by

$$\frac{\partial \theta}{\partial x} = k(x_1), \tag{3.2}$$

$$\frac{\partial \theta}{\partial t} = -\omega. \tag{3.3}$$

The dimensional wavenumber and frequency are

$$\left.\begin{aligned} k^* &= \frac{k}{D} \\ \omega^* &= \frac{U_{\max}}{D}\,\omega \end{aligned}\right\}. \tag{3.4}$$

Since we are studying the spatial growth rate under the influence of slow streamwise variation of the basic flow, the frequency ω is assumed to be a constant so that the temporal growth rate is excluded. This may be viewed as forcing a wave with a fixed period (frequency) at a certain x_1 and allowing it to propagate downstream. The wavenumber k can be written, following the suggestion of Benney and Rosenblat (1964), as

$$k = \sum_{n=0}^{\infty} \epsilon^n k_n = k_0 + \epsilon k_1 + \epsilon^2 k_2 + \cdots \tag{3.5}$$

and ϕ can be expanded asymptotically as

$$\phi = \sum_{n=0}^{\infty} \epsilon^n \phi_n = \phi_0 + \epsilon\phi_1 + \epsilon^2\phi_2 + \cdots. \tag{3.6}$$

In order to eliminate some difficulties in the mathematical formulation, the phase θ is treated as an independent variable in place of x, as proposed by Nayfeh et al. (1974). The following relations, which hold to $O(\epsilon)$ accuracy, can be derived with the chain rule:

$$\left.\begin{aligned} \frac{\partial}{\partial x} &\to k_0 \frac{\partial}{\partial \theta} + \epsilon\left(\frac{\partial}{\partial x_1} + k_1 \frac{\partial}{\partial \theta}\right) \\ \frac{\partial}{\partial t} &\to -\omega \frac{\partial}{\partial \theta} \\ \frac{\partial^2}{\partial x^2} &\to k_0^2 \frac{\partial^2}{\partial \theta^2} \\ &\quad + \epsilon\left(2k_0 \frac{\partial^2}{\partial \theta \partial x_1} + 2k_0 k_1 \frac{\partial^2}{\partial \theta^2} + \frac{k_0}{\partial x_1}\frac{\partial^2}{\partial \theta}\right) \end{aligned}\right\}. \tag{3.7}$$

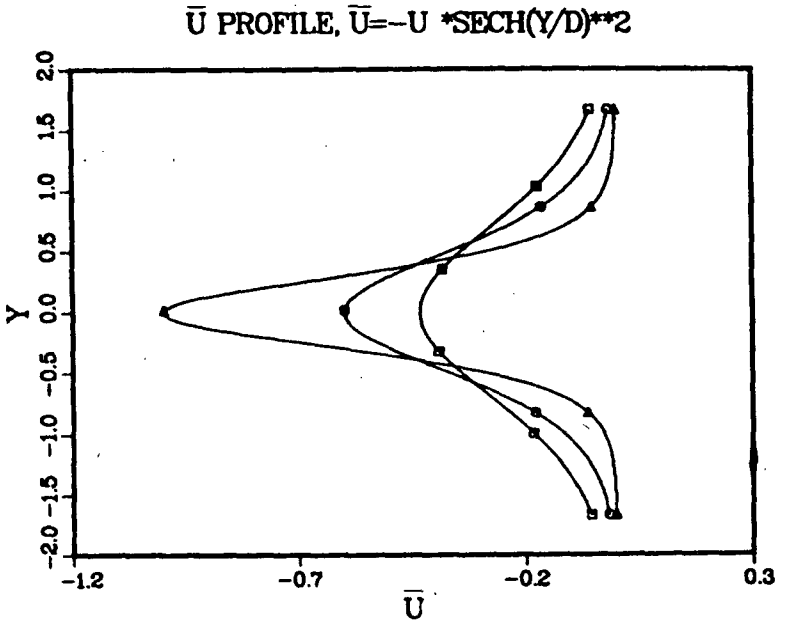

FIG. 1. The Bickley Jet $\bar{U}$ profile [Eq. (2.7)] at three streamwise locations. The □ curve is the profile at $x_1 = \pm 2.0$, the ○ curve is at $x_1 = \pm 1.0$, and the △ curve is at $x_1 = 0$. Both the width and the maximum speed of the jet change streamwise.

Now use (3.5) and (3.6) in (3.1), and then substitute into (2.1) and (2.3). With the help of (3.7) and (2.2), we obtain a sequence of equations for different orders of ϵ.

O(1) problem:

$$L(\phi_0) = \frac{\partial^2 \phi_0}{\partial y^2} - k_0^2 \phi_0 - \frac{k_0 \phi_0 (\bar{U}_{yy} - \beta)}{(k_0 \bar{U} - \omega - i\lambda)} = 0 \quad (3.8)$$

$$\phi_0 = 0 \quad \text{at} \quad y = \pm Y. \quad (3.9)$$

The O(1) problem is identical to the problem when $\epsilon = 0$, i.e., parallel flow. For each x_1, $\bar{U}$ and $\bar{U}_{yy}$ are prescribed by (2.7), and Eqs. (3.8)–(3.9) give an eigenvalue problem. If ω is replaced by kc, where c is the phase speed, the conventional temporal barotropic instability is obtained by setting k as a constant and solving for complex c (Kuo, 1973). In our study, where ω is constant, k is the eigenvalue and ϕ the eigenfunction. The basic flow is spatially unstable when k is complex. The imaginary part of k gives us the spatial growth rate while the real part is the local wavenumber.

Since Eqs. (3.8) and (3.9) constitute a nonlinear problem with the eigenvalue k, an iterative shooting method for the complex eigenvalue problem is employed. The fourth-order Runge–Kutta–Gill method is used to integrate Eq. (3.8) from one boundary to the other. The first guess for the eigenvalue is chosen from the range of interest. Only six or seven iterations are required for the solution to converge to the specified boundary condition with absolute error less than 10^{-4}. For each x_1 that has a different $\bar{U}$ profile, the eigenvalue obtained from the previous point is used as the initial guess. With this first guess only two or three iterations are required.

O(ϵ) problem:

$$\begin{aligned} L(\phi_1) &= \frac{\partial^2 \phi_1}{\partial y^2} - k_0^2 \phi_1 - \frac{k_0 \phi_1 (\bar{U}_{yy} - \beta)}{(k_0 \bar{U} - \omega - i\lambda)}, \\ &= F, \\ &= \frac{1}{(k_0 \bar{U} - \omega - i\lambda) i} \Big\{ (3k_0^2 \bar{U} - 2\omega k_0 + \bar{U}_{yy} - \beta - i\lambda 2k_0) \\ &\quad \times \frac{\partial \phi_0}{\partial x_1} + (3\bar{U} k_0 - \omega - i\lambda) \phi_0 \frac{\partial k_0}{\partial x_1} - \bar{U} \frac{\partial^3 \phi_0}{\partial y^2 \partial x_1} \\ &\quad + \bar{V} k_0^2 \frac{\partial \phi_0}{\partial y} - \bar{V} \frac{\partial^3 \phi_0}{\partial y^3} + \frac{\partial \phi_0}{\partial y} \bar{V}_{yy} \\ &\quad + ik_1 \Big(3\bar{U} k_0^2 \phi_0 - 2\omega k_0 \phi_0 - \bar{U} \frac{\partial^2 \phi_0}{\partial y^2} \\ &\qquad + \phi_0 \bar{U}_{yy} - \beta \phi_0 - 2i\lambda k_0 \phi_0 \Big) \Big\}, \quad (3.10) \end{aligned}$$

$$\phi_1 = 0 \quad \text{at} \quad y = \pm Y. \quad (3.11)$$

Since the left-hand side operator of (3.10) is the same as in (3.8) for the O(1) problem, (3.10) has nontrivial homogeneous solutions that are proportional to ϕ_0. In order to remove secularity so that the multiple expansion can remain valid, a solvability condition has to be imposed on (3.10). (See Nayfeh, 1981). The condition is

$$\int_{-Y}^{Y} F \phi_0^* dy = 0 \quad (3.12)$$

where ϕ_0^* is the solution of the adjoint equation of the O(1) problem. Since the operator L in the O(1) problem is self-adjoint, $L = L^*$; therefore, $\phi_0 = \phi_0^*$.

The unknown k_1, as well as k_0, is independent of y. Rearrangement of (3.12) gives us the following equation for k_1:

$$k_1 = \frac{H_1}{H_2}, \quad (3.13)$$

where

$$\begin{aligned} H_1 &= i \int_{-Y}^{Y} \frac{\phi_0^*}{(k_0 \bar{U} - \omega - i\lambda)} \Big\{ \frac{\partial \phi_0}{\partial x_1} (3k_0^2 \bar{U} - 2\omega k_0 + \bar{U}_{yy} \\ &\quad - \beta - 2i\lambda k_0) + (3\bar{U} k_0 - \omega - i\lambda) \frac{\partial k_0}{\partial x_1} \phi_0 - \bar{U} \frac{\partial^3 \phi_0}{\partial x_1 \partial y^2} \\ &\quad + \bar{V} k_0^2 \frac{\partial \phi_0}{\partial y} - \bar{V} \frac{\partial^3 \phi_0}{\partial y^3} + \frac{\partial \phi_0}{\partial y} \bar{V}_{yy} \Big\} dy \quad (3.13a) \end{aligned}$$

$$\begin{aligned} H_2 &= \int_{-Y}^{Y} \frac{\phi_0^*}{(k_0 \bar{U} - \omega - i\lambda)} \Big(3\bar{U} k_0^2 \phi_0 - 2\omega k_0 \phi_0 \\ &\quad - \bar{U} \frac{\partial^2 \phi_0}{\partial y^2} + \phi_0 \bar{U}_{yy} - \beta \phi_0 - 2i\lambda k_0 \phi_0 \Big) dy. \quad (3.13b) \end{aligned}$$

For nonparallel flow, the spatial growth rate is, to O(ϵ),

$$\mathrm{Im}(k_0 + \epsilon k_1) \quad (3.14)$$

and the local wavenumber is

$$\mathrm{Re}(k_0 + \epsilon k_1). \quad (3.15)$$

In order to obtain k_1 as a function of x_1, terms such as $\partial \phi_0 / \partial x_1$, $\partial k_0 / \partial x_1$ and $\partial^3 \phi_0 / \partial x_1 \partial y^2$ in (3.13) have to be known. They can be obtained by finite difference methods since ϕ_0, k_0 are known at each point (x_1, y). An alternate way suggested by Nayfeh et al. (1974) is to take $\partial / \partial x_1$ of (3.8). This leads to an equation

$$L\left(\frac{\partial \phi_0}{\partial x_1}\right) = G\left(\frac{\partial k_0}{\partial x_1}, k_0, \phi_0, \text{etc.}\right). \quad (3.16)$$

Equation (3.16) has the same structure as Eq. (3.10), so the same solvability condition is required, i.e.,

$$\int_{-Y}^{Y} \phi_0^* G dy = 0. \quad (3.17)$$

An equation for $\partial k_0 / \partial x_1$ can be obtained with similar form to (3.13), and then $\partial \phi_0 / \partial x_1$ can be obtained from (3.16). When the finite difference method and the analytical method are compared, the results are very close.

TABLE 1. Temporal and spatial growth rates.

Parameter	Temporal growth rate	Spatial growth rate
wave structure	$e^{i(kx-\omega t)}$	$e^{i(kx-\omega t)}$
wavenumber	$k = k_r$	$k = k_r + ik_i$
frequency	$\omega = \omega_r + i\omega_i$	$\omega = \omega_r$
growth rate	ω_i (temporal)	k_i (spatial)
phase speed c	ω_r/k_r	ω_r/k_r

4. Temporal growth rate versus spatial growth rate

Before discussing the results from the present study, it is necessary to examine the functional relationship between the temporal growth rate and the spatial growth rate. In TWC, the parallel-flow spatial growth rate was not obtained directly, but transformed from the temporal growth rate. This discussion will lead to an important modification of the conclusions in TWC as well as those in the nonlinear numerical study by Williams et al. (1984). The basic procedures and assumptions in obtaining temporal and spatial growth rates are different, as is indicated in Table 1.

Various efforts have been made to determine a relationship that converts one type of growth rate into another. In an experimental investigation of the boundary layer over a flat plate, a simple relation was formulated by Schubauer and Skramstad (1943) in order to compare the measured amplification rates (spatial growth rates) with the temporal growth rates given by theory. They related the temporal growth rate to the spatial growth rate with the chain rule as follows:

$$k_i = -\frac{\omega_i}{c_r} \tag{4.1}$$

where k_i is spatial growth rate, ω_i is the temporal growth rate, and $c_r = dx/dt$ is the phase speed. Gaster (1965) demonstrated that the transformation between the two kinds of growth rates, which uses the phase speed, introduces errors that are not negligible. However, Schubauer and Skramstad did make their comparison and some correlation was found.

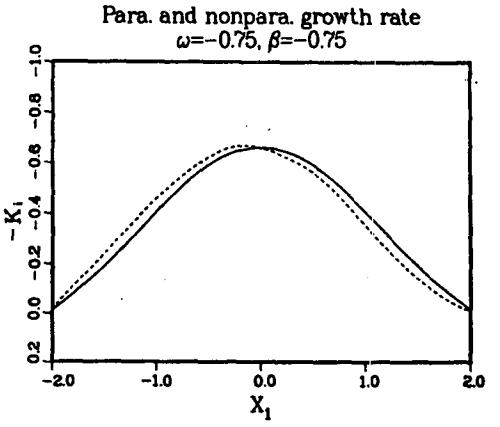

FIG. 3. The spatial growth rate corresponding to the Bickley Jet profile [Eq. (2.7)], whose streamwise variation is described by (2.9) and (2.10). The solid line is the spatial growth rate for the parallel flow, and the dashed line is the spatial growth rate for the nonparallel flow.

Gaster (1962) used a Taylor series expansion to show that when the amplification rate is small, a transformation by means of the group velocity can be formulated. In a study of the nonparallel flow stability for two- and three-dimensional flow, Nayfeh and Padhye (1979) derived a formula for the transformation between growth rates. Their formula differs from Gaster's in two respects. First, the complex group velocity is used instead of the real group velocity, which is used in Gaster's formula. Second, a correction to the wavenumber (frequency) must be added when transforming from temporal (spatial) to spatial (temporal) growth rates.

Calculations using Nayfeh and Padhye's formula [1979, Eq. (41)] show that when the amplification rate is small (i.e., the imaginary part of the eigenvalue is

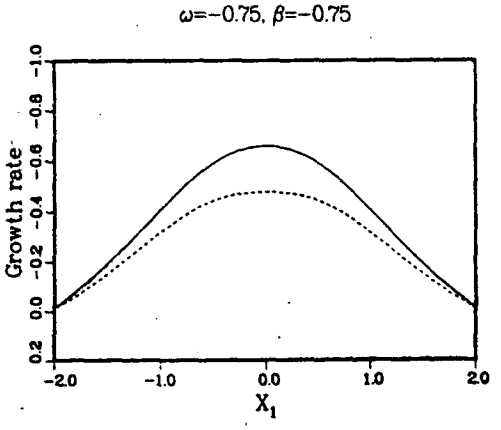

FIG. 2. Spatial growth rate for (solid line) parallel flow for $\omega = -0.75$, $\beta = -0.75$; and (dashed line) obtained using Eq. (4.1).

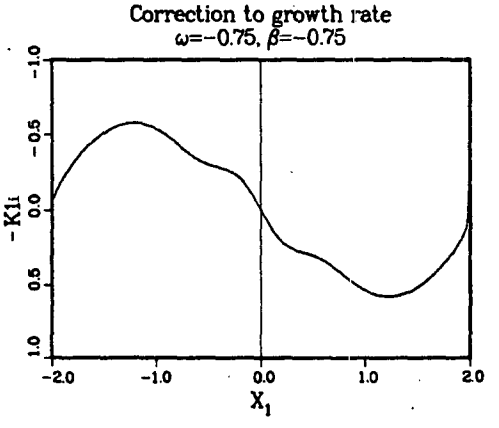

FIG. 4. The imaginary part of k_1, or the $O(\epsilon)$ correction to the spatial growth rate at each streamwise location.

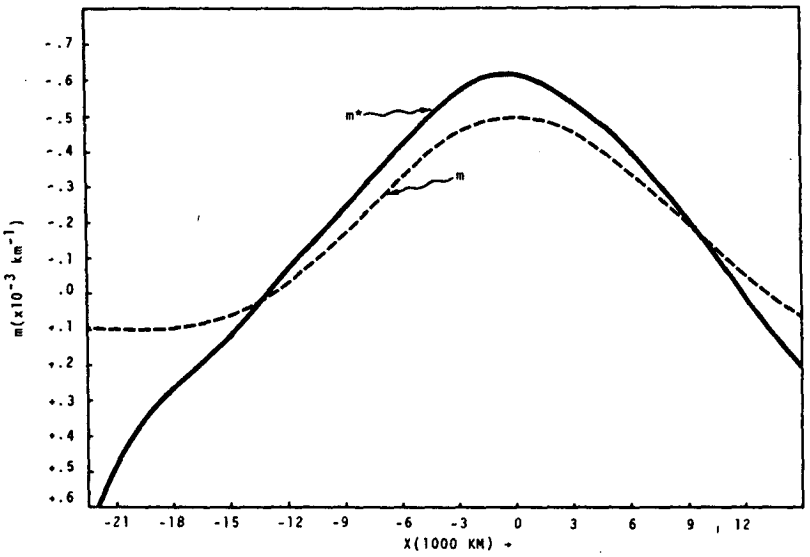

FIG. 5. Experiment 1 (from TWC): spatial growth rates $m(x)$ from the parallel flow model and $m^*(x)$ from the complete numerical model. When $m < 0$ there is downstream growth. (Adopted from TWC.)

small), the transformation is very accurate. This is consistent with results given in Tables 1 and 2 by Nayfeh and Padhye (1979), where all the cases are also for small amplification. When the amplification rate increases from 0.013 to 0.65, the error increases almost linearly from 0.4% to 20%. Apparently, a small amplification rate is required to obtain accurate results using Nayfeh and Padhye's (1979) formula.

In TWC, a simple mechanistic model was formulated that leads to Eq. (4.1). As discussed above, the use of Eq. (4.1) in TWC to transform the spatial growth rates from temporal growth rate for the parallel flow introduces significant errors.

Figure 2 contains the spatial growth rate as a function of x_1 for $\bar{U}$ profiles, which are described by Eqs. (2.7), (2.9) and (2.10). The nondimensional parameter settings $\omega = -0.75$, $\beta = -0.75$ correspond to the case studied in TWC for a period of 3.25 days and with the central latitude at 10°N. The solid line is obtained by directly solving the parallel flow equations at each point in x_1 for the complex wavenumber k as the eigenvalue. The spatial growth rate is the imaginary part of k. The dashed line is obtained as in TWC by solving the parallel flow equations for the complex frequency as the eigenvalue and then using Eq. (4.1) to calculate the spatial growth rate.

Figure 2 shows that in the maximum growth rate region, the use of Eq. (4.1) underestimates the true spatial growth rate by 27%. A similar percentage difference was also obtained by Michalke (1965). In TWC, Eq. (4.1) was evaluated with the same wavenumbers as those from their complete nonparallel numerical model where the spatial growth rates were measured directly. An alternative is to iterate the wavenumber until the same frequency is obtained. Both methods were used in a later paper by Williams et al. (1984). In the present study it is found that keeping the same frequency in the transformation gives an improvement in growth rate of 2%–4%, compared to the transformation retaining the same wavenumber. Clearly this improvement is not significant. The percentage error that results from the use of Eq. (4.1) increases slightly from 20% to 27% when the growth rate increases from 0.013 to 0.65, respectively.

Detailed discussion concerning the transformation of the growth rate is beyond the scope of the present

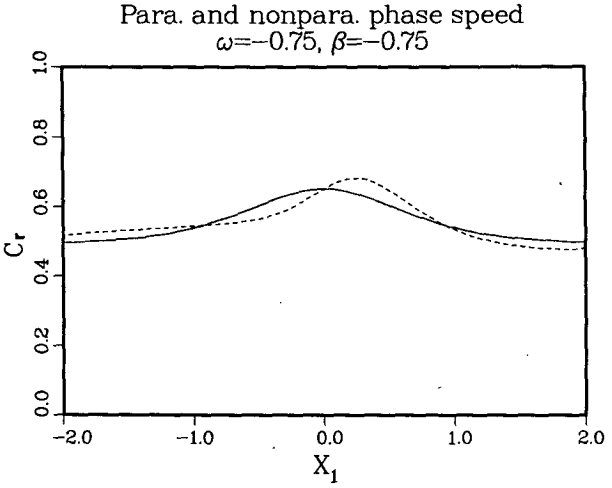

FIG. 6. The phase speed for the case whose spatial growth rate is shown in Fig. 3. Solid line: parallel phase speed; dashed line: nonparallel phase speed.

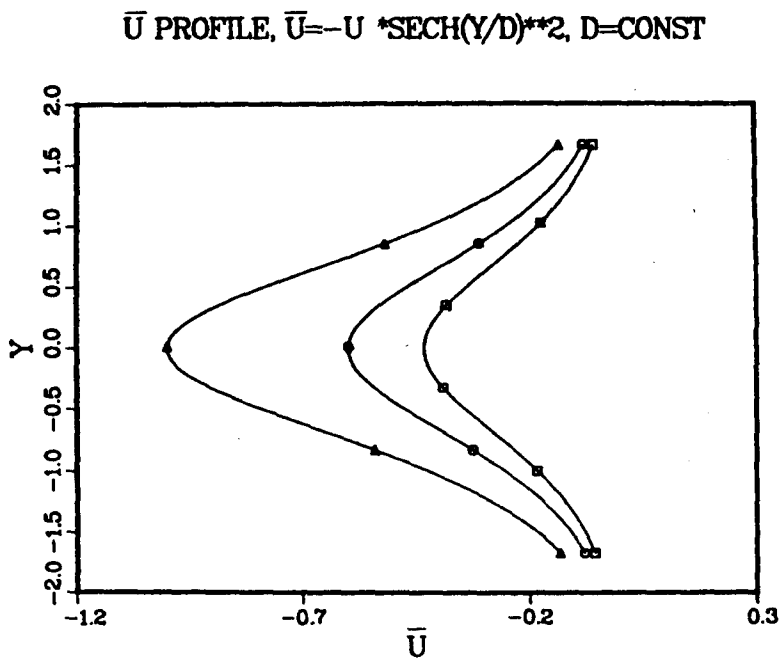

FIG. 7. As in Fig. 1 except the width of the jet is kept the same.

study and is presented in a separate paper by the authors (Peng and Williams, 1986).

5. Results

In this section we will compare the parallel and nonparallel solutions in order to determine the influence of nonparallel effects on spatial instability. Within each diagram in this section, the solid line refers to the variables for pure parallel flow, which are obtained from the O(1) problem; the dashed line refers to the variables for nonparallel flow to O(ϵ). The positive imaginary wavenumber gives downstream amplification of the wave amplitude when the propagation is from east to west. The downstream growth rate is $-k_i$, which is plotted throughout the text. The parallel and nonparallel growth rates shown in Fig. 3 are for the parameter values used in Fig. 2. The parallel flow growth rate changes symmetrically with respect to $x_1 = 0$, as is expected from symmetric streamwise variation of the basic flow. The O(ϵ) correction to the wavenumber, k_1, which is given in Fig. 4, is antisymmetric with respect to $x_1 = 0$. Examining (3.13), one observes that k_1 is proportional to terms such as $\partial\phi_0/\partial x_1$, $\partial k_0/\partial x_1$, $\bar{V}$, etc., all of which are the first derivatives of ϕ_0, k_0, $\bar{\psi}$, etc. Since ϕ_0, k_0, $\bar{\psi}$ are symmetric with respect to $x_1 = 0$, their first-order derivatives with respect to x_1 are antisymmetric. Note that if we multiply the curve in Fig.

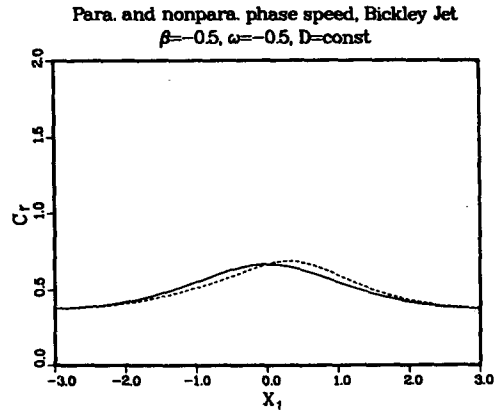

FIG. 8. The parallel (solid line) and the nonparallel (dashed line) phase speed for the jet profile shown in Fig. 7.

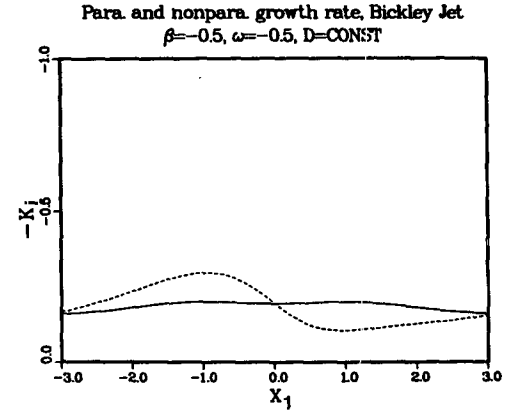

FIG. 9. As in Fig. 8 except for the spatial growth rate for the jet profile.

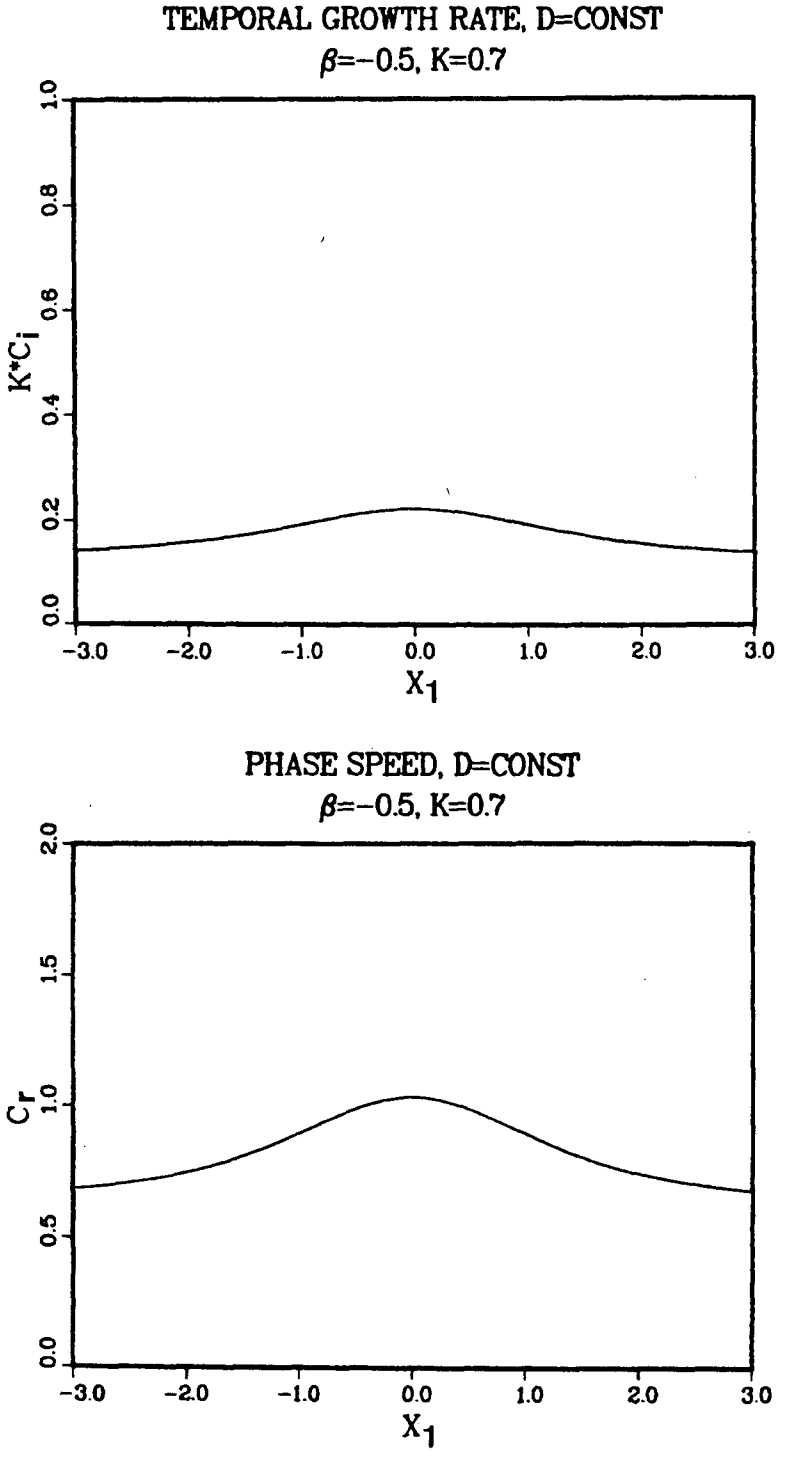

FIG. 10. (a) The temporal growth rate from parallel theory for the jet profile shown in Fig. 7. (b) The corresponding phase speed.

4 by ϵ, we obtain the difference between the nonparallel and the parallel solutions in Fig. 3. These figures show that the maximum growth rate region is shifted downstream from the location predicted by the parallel flow instability. At $x_1 = 0$ where the parallel growth rate is maximum, all the first-order derivatives are zero. Therefore, $k_1 = 0$ at $x_1 = 0$ and the growth rates are the same for parallel and nonparallel flows.

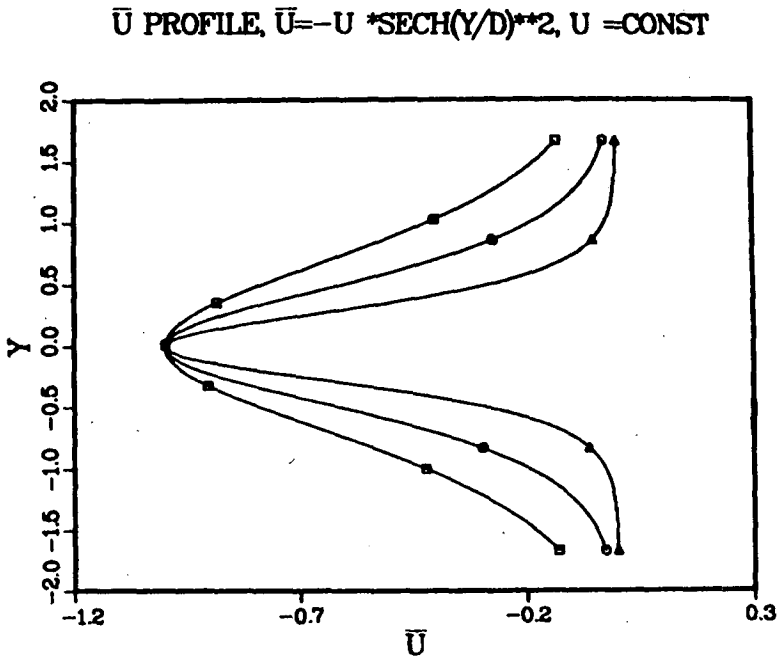

FIG. 11. As in Fig. 1 except the maximum wind speed is kept constant so that only the width of the jet varies.

The downstream shifting of the location of maximum growth rate was observed in TWC and by Williams et al. (1984). As the disturbance propagates downstream in a nonparallel flow, the disturbance structure lags with respect to the parallel flow disturbance structure. Therefore, the profile for spatial growth rate in the streamwise direction is shifted downstream from the profile calculated from the parallel flow. The dynamic damping observed in the numerical result in TWC, which was due to continuous spectrum solutions (Case, 1960), is absent in the normal-mode solutions derived in this paper. Moreover, as shown in Fig. 5, which is adopted from TWC, the nonparallel growth rate is approximately 25% higher than the parallel growth rate calculated by them. This increase is not observed in the present study. As explained in section 4, the parallel growth rate calculated in TWC underestimates the true growth rate by approximately 27%. If this percentage is added to the parallel growth rate in Fig. 5, the results from the present analytical study and from the numerical study (TWC) are consistent. Therefore, there is no overall increase of the growth rate for nonparallel flow at the point where the parallel flow growth rate is a maximum.

The phase speed of the disturbance is

$$c=\frac{\omega}{k_r} \tag{5.1}$$

where k_r is the local wavenumber. For parallel flow, k_r equals real(k_0), and for nonparallel flow, k_r = real(k_0 + ϵk_1). The phase speed for the case shown in Fig. 3 is plotted in Fig. 6. Upstream from the maximum growth rate point for parallel flow, i.e., where $x_1 = 0$, the disturbance moves faster than predicted by the parallel flow and slower downstream. It is postulated that the difference between growth rate calculated from parallel flow and nonparallel flow is closely related to the relative phase speed between them.

Equation (4.1) implies that if the phase speed for disturbance in the nonparallel flow is faster than predicted by parallel flow, the disturbance will have less time to grow according to the local instability so that the growth rate will be smaller than that predicted by parallel flow. The opposite holds for a disturbance that propagates slower than that predicted by parallel flow. Therefore, a disturbance with a faster (slower) phase speed will have smaller (larger) spatial growth rate. An experiment described in TWC in which a constant velocity U_0 is added to the mean flow did show a significant reduction in local spatial growth rate. This advective effect also produced more downstream shifting of the spatial growth rate profile.

This discussion is based primarily on the approximate expression for the spatial growth (4.1). However, it is believed that this formula gives the correct dependence on the phase speed. In order to gain more insight into the influence of the phase speed rate on the spatial growth, two cases will be considered. A jet profile with a constant half width is used in the first case. The change of the basic flow shear is due to the streamwise change in the speed of the jet. Mathematically, d is set to a constant and only U varies with x_1 in (2.7). Profiles of $\bar{U}$ at several locations are shown in Fig. 7. We shall

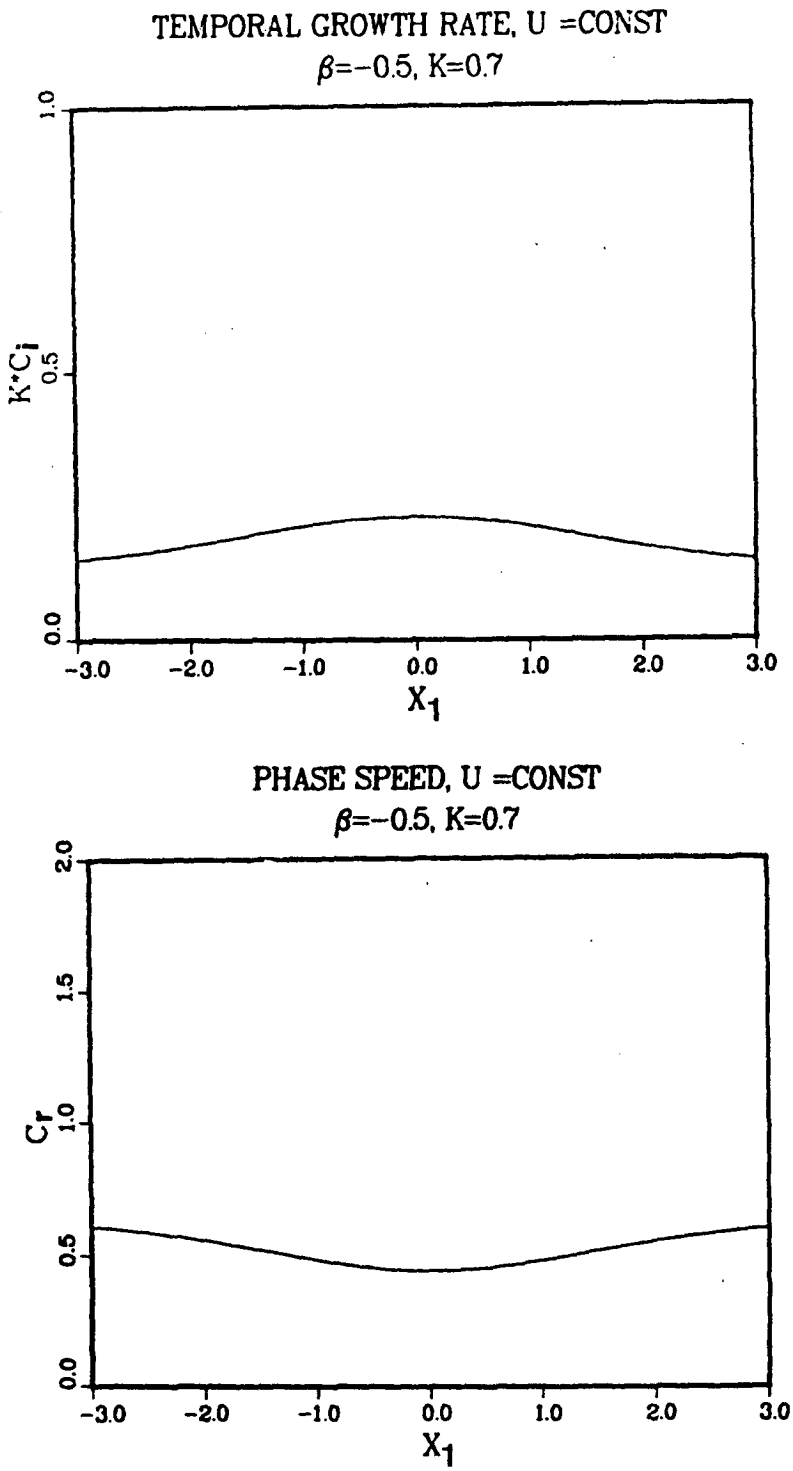

FIG. 12. As in Fig. 10 except corresponding to Fig. 11.

first examine the phase speed of the disturbance that is plotted in Fig. 8. The phase speed is larger for nonparallel flow upstream of $x_1 = 0$ and smaller downstream, as in the previous case (Fig. 6). Therefore, the spatial growth rate for nonparallel flow would be smaller than the parallel flow upstream and larger downstream, as indicated in Fig. 9. Notice that the growth rate for the parallel flow is nearly uniform ir-

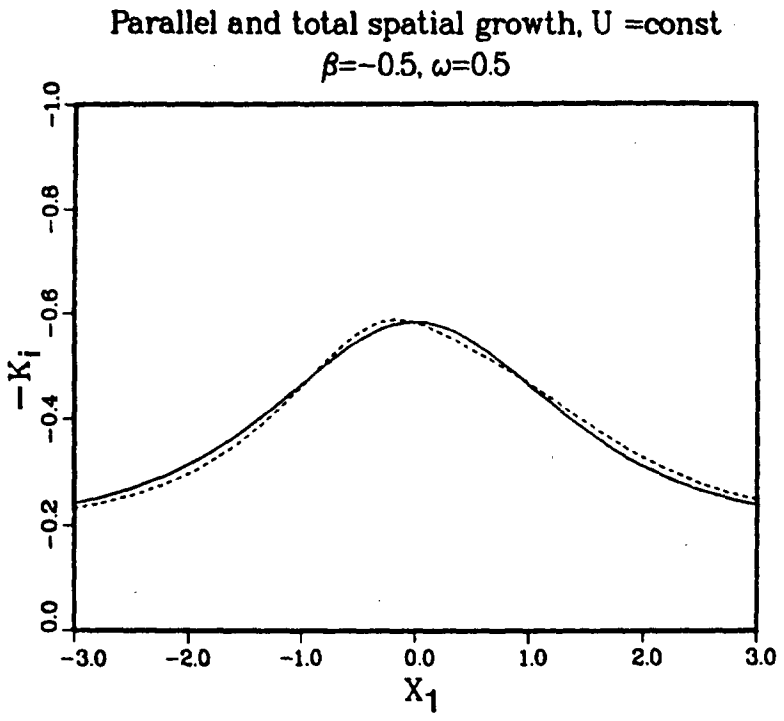

FIG. 13. As in Fig. 9 except corresponding to Fig. 11.

respective of the large variation of the jet strength. This seems to contradict the notion that barotropic instability increases as the north–south shear of the basic flow increases. However, an examination of Eq. (4.1) reveals that for spatial instability, the growth rate is also related to the phase speed of the disturbance. Even though the temporal growth rate increases in proportion to the increase of the mean flow shear, as shown

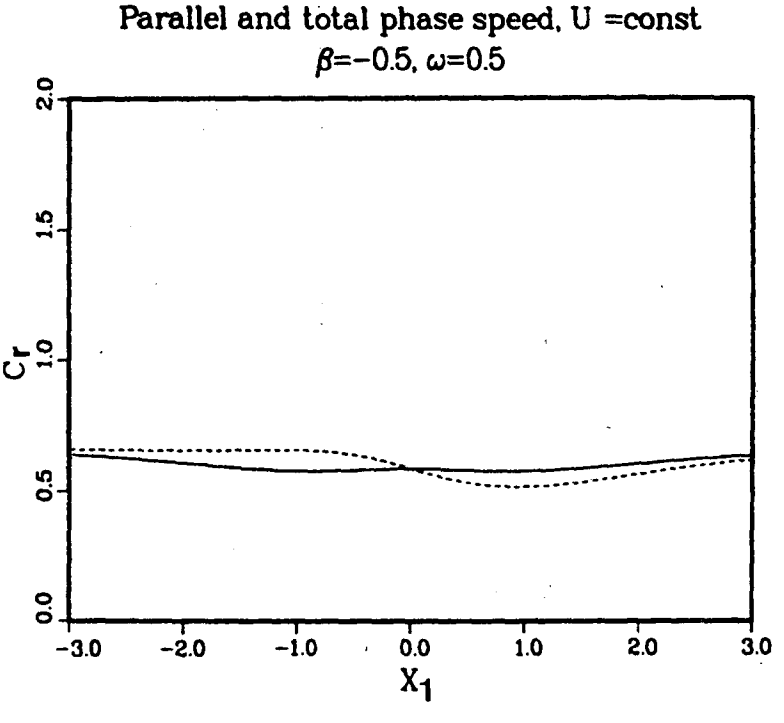

FIG. 14. As in Fig. 8 except corresponding to Fig. 11.

in Fig. 10a, the accompanying increase of the phase speed (Fig. 10b) results in a small change in the spatial growth rate. Therefore, from the point of view of spatial growth rate, which is more appropriate in a nonparallel flow, the maximum shear region is not necessarily the most unstable region.

In the second case, the jet profile is considered to have a constant maximum speed. The increase of the shear is due to the decrease of the jet half width. This is prescribed by setting U equal to a constant and by allowing only d to vary in (2.7). Mean flow profiles of $\bar{U}$ are displayed in Fig. 11 for the same locations as in Fig. 7. For this kind of variation, the temporal growth rate increases while the phase speed decreases with the increase of the basic flow shear. (See Figs. 12a,b.) This leads to a substantial variation of the spatial growth rate for parallel flow. The nonparallel spatial growth rate is quite different from previous cases when compared to the parallel flow spatial growth (Fig. 13). In Fig. 14, the nonparallel phase speed is slower than the parallel phase speed upstream of $x_1 = 0$ and faster downstream. If the shifting of nonparallel growth rate from that predicted by the parallel flow is due solely to the phase speed differences between the parallel and nonparallel flows, the nonparallel growth rate would be larger upstream of $x_1 = 0$ and smaller downstream. However, this is only true in part of the region. The maximum growth rate region for nonparallel flow is still shifted downstream, which should be expected by the lag effect proposed in TWC. This indicates that the shifting is due to the combination of the two effects: one involves the lag mechanism, and the other depends on the phase speed difference between the parallel and nonparallel flows.

The example shown in Fig. 3, which is comparable to the case considered by TWC, indicates a relatively small difference between parallel and nonparallel flow. This is not a general result, as will be demonstrated with an example. Figure 15 has the same conditions as in Fig. 3 except that the frequency of the disturbance

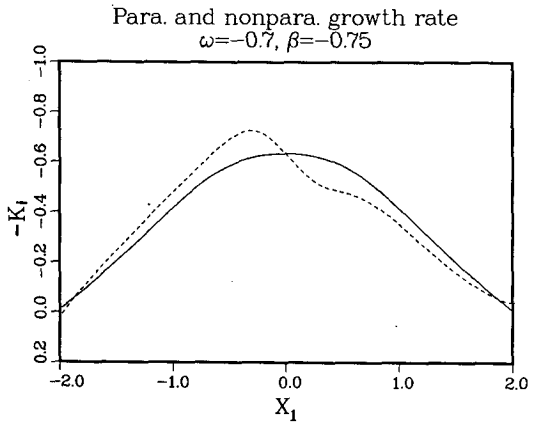

FIG. 15. As in Fig. 3 except $\omega = -0.7$.

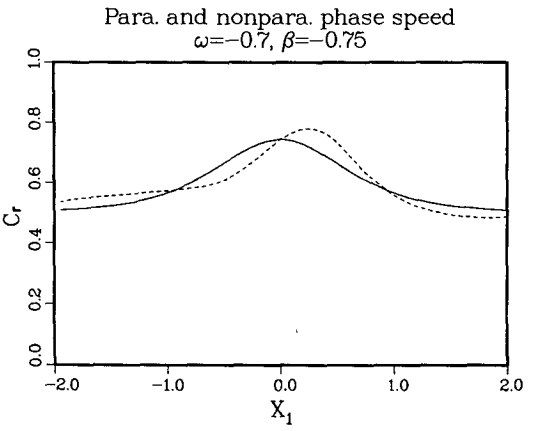

FIG. 16. As in Fig. 6 except $\omega = -0.7$.

is smaller; it corresponds to a period of 3.5 days whereas the frequency in Fig. 3 corresponds to period of 3.25 days. The stronger asymmetry of the growth rate curve in Fig. 15 compared to Fig. 3 is due to the larger phase speed shown in Fig. 16, which gives a larger lag effect. Differences of the phase speed between parallel and nonparallel flow are also slightly larger in this case. Further increases in the period lead to similar results.

6. Concluding remarks

In this study a two-scale expansion is used to analyze the linear instability of a barotropic jet that varies downstream. A small parameter ϵ is introduced to measure the nonparallelism of the mean flow. The O(1) problem gives the parallel flow equation at each point in the streamwise direction. The O(ϵ) problem gives the correction to the spatial growth rate due to the nonparallelism, which is proportional to the first streamwise derivative of the properties from the O(1) problem. This O(ϵ) correction causes the downstream shifting of the spatial growth rate profile for nonparallel flow relative to that of the parallel flow obtained from the O(1) problem.

Results obtained here are consistent with the numerical studies by TWC after a necessary modification of their parallel flow growth rates. In the present analysis, only the normal mode solutions are considered, whereas in TWC's numerical study the continuous spectrum effects are also included. The closeness of these two results indicates that the normal modes accurately describe the solution in the region of growth. The rapid decay of the growth rate near the outflow region, which was seen in the numerical solution, is not present in the analytical solution. The decay in the numerical solution appears to have been caused by continuous spectrum effects.

Physically, the difference between the nonparallel flow solutions and the parallel flow solutions are caused by two effects. The first one, which has been discussed by TWC, is the lag effect. When the disturbance propagates through a mean flow that varies in streamwise

direction, the disturbance lags in adjusting its structure to the local instability properties. This lagging causes a downstream shifting of the spatial growth rate profile. The second effect is due to the influence of the phase speed on the spatial growth rate. If the phase speed in the nonparallel flow is faster than that predicted by the parallel flow, the disturbance will move further in a given time interval, and therefore, the spatial growth rate will be reduced.

In a streamwise varying mean flow, it is more appropriate to study the spatial growth rate than the temporal growth rate. As is commonly known, the temporal growth rate is proportional to the cross-stream shear of the unstable zonal flow. Since the spatial growth rate depends on the propagating phase speed, the maximum shear region is not necessarily the region of the maximum spatial growth rate. This is an important consideration in the application of instability theories to synoptic examples.

Acknowledgments. The authors wish to thank Professor C.-P. Chang for reading the manuscript and for useful discussions on the research. The first author was supported by a National Research Council Associateship. The NRC Associate Program is sponsored by the Naval Postgraduate School Foundation Research Program, which is funded by the Chief of Navy Material. This research was also supported by the Division of Atmospheric Sciences, National Science Foundation under Grant ATM 83-15175. The manuscript was carefully typed by Miss K. Lee and the numerical computations were carried out at the W. R. Church Computer Center at the Naval Postgraduate School.

REFERENCES

Benney, D. J., and S. Rosenblat, 1964: Stability of spatially varying and time-dependent flows. *Phys. Fluids,* **7,** 1385–1386.

Case, K. M., 1960: Stability of plane couette flow. *Phys. Fluids,* **3,** 143–148.

Drazin, P. G., 1974: On a model of instability of a slowly-varying flow. *Quart. J. Mech. Appl. Math.,* **27,** 69–86.

Gaster, M., 1962: A note on the relation between temporally-increasing and spatially-increasing disturbances in hydrodynamics instability. *J. Fluid Mech.,* **14,** 222–224.

——, 1965: The role of spatially growing waves in the theory of hydrodynamic stability. *Prog. Aerospace Sci.,* **6,** 251–270.

Haltiner, G. J., and R. T. Williams, 1980: *Numerical Prediction and Dynamic Meteorology.* Wiley & Sons, 477 pp.

Krishnamurti, T. N., 1961: The subtropical jet stream of winter. *J. Meteor.,* **18,** 172–191.

Kuo, H. L., 1973: Dynamics of quasi-geostrophic flows and instability theory. *Advances in Applied Mechanics,* **Vol. 13,** Pergamon, 247–330.

Merkine, L.-O., 1977: Convective and absolute instability of baroclinic eddies. *Geophys. Astrophys. Fluid Dyn.,* **9,** 129–157.

——, and R. Balgovind, 1983: Barotropic instability of weakly nonparallel zonal flows. *Geophys. Astrophys. Fluid Dyn.,* **25,** 157–190.

Michalke, A., 1965: On spatially growing disturbances in an inviscid shear layer. *J. Fluid Mech.,* **23,** 521–544.

Nayfeh, A. H., 1981: *Introduction to Perturbation Techniques.* Wiley & Sons, 519 pp.

——, and A. Padhye, 1979: Relation between temporal and spatial stability in three-dimensional flows. *AIAA J.,* **17,** 1084–1090.

——, W. S. Saric and D. T. Mook, 1974: Stability of nonparallel flows. *Arch. Mech.,* **26,** 401–406.

Pedlosky, J., 1976: *Geophysical Fluid Dynamics.* Springer-Verlag, 624 pp.

Peng, M. S., and R. T. Williams, 1986: A note on the relation between temporal and spatial growth rate. Submitted to *J. Atmos. Sci.*

Saric, W. S., and A. H. Nayfeh, 1975: Nonparallel stability of boundary-layer flows. *Phys. Fluids,* **18,** 945–950.

Schubauer, G. B., and H. K. Skramstad, 1943: Laminar boundary layer oscillations and transition on a flat plate. NACA Advanced Confidential Rep., April 1943, or 1947, *J. Res. Nat. Bur. Stand.,* **38,** 251–292.

Tupaz, J. B., R. T. Williams and C.-P. Chang, 1978: A numerical study of barotropic instability in a zonally varying easterly jet. *J. Atmos. Sci.,* **35,** 1265–1280.

Williams, R. T., H. Lim and C.-P. Chang, 1984: Nonlinear and linear effects in an easterly jet with downstream variation. *J. Atmos. Sci.,* **41,** 621–636.